

University of Nebraska - Lincoln

DigitalCommons@University of Nebraska - Lincoln

Papers in Natural Resources

Natural Resources, School of

2021

Reconstruction of pre-Illinoian ice margins and glaciotectonic structures from airborne electromagnetic (AEM) surveys at the western limit of Laurentide glaciation, Midcontinent U.S.A.

Jesse T. Korus

University of Nebraska-Lincoln, jkorus3@unl.edu

Robert M. Joeckel

University of Nebraska-Lincoln, rjoeckel3@unl.edu

Jared D. Abraham

Aqua-Geo Frameworks LLC, Fort Laramie, WY, jabraham@aquageoframeworks.com

Anne-Sophie Høyer

Geological Survey of Denmark and Greenland, ahc@geus.dk

Flemming Jørgensen

Central Denmark Region, Viborg, Denmark, fljoer@rm.dk

Follow this and additional works at: <https://digitalcommons.unl.edu/natrespapers>



Part of the [Natural Resources and Conservation Commons](#), [Natural Resources Management and Policy Commons](#), and the [Other Environmental Sciences Commons](#)

Korus, Jesse T.; Joeckel, Robert M.; Abraham, Jared D.; Høyer, Anne-Sophie; and Jørgensen, Flemming, "Reconstruction of pre-Illinoian ice margins and glaciotectonic structures from airborne electromagnetic (AEM) surveys at the western limit of Laurentide glaciation, Midcontinent U.S.A." (2021). *Papers in Natural Resources*. 1480.

<https://digitalcommons.unl.edu/natrespapers/1480>

This Article is brought to you for free and open access by the Natural Resources, School of at DigitalCommons@University of Nebraska - Lincoln. It has been accepted for inclusion in Papers in Natural Resources by an authorized administrator of DigitalCommons@University of Nebraska - Lincoln.



Reconstruction of pre-Illinoian ice margins and glaciotectonic structures from airborne ElectroMagnetic (AEM) surveys at the western limit of Laurentide glaciation, Midcontinent U.S.A.



Jesse T. Korus^{a,*}, R.M. Joeckel^{a,b}, Jared D. Abraham^c, Anne-Sophie Høyer^d, Flemming Jørgensen^e

^a Conservation and Survey Division, School of Natural Resources, 3310 Holdrege Street, University of Nebraska–Lincoln, Lincoln, NE, USA

^b Department of Earth and Atmospheric Sciences, University of Nebraska–Lincoln, Lincoln, NE, USA

^c Aqua-Geo Frameworks LLC, 10848 Ridge Road, Fort Laramie, WY, 82212-7614, USA

^d Geological Survey of Denmark and Greenland, CF Møllers Alle 8, Building 8, 8000, Aarhus C, Denmark

^e Central Denmark Region, Skottenborg 26, 8800, Viborg, Denmark

ARTICLE INFO

Keywords:

Glaciotectonics
Glaciation
Glacial limit
Geophysics
Laurentide
Pre-Illinoian

ABSTRACT

Early and early Middle Pleistocene glaciations in midcontinental USA are poorly understood relative to more recent Illinoian and Wisconsinan glaciations, largely because pre-Illinoian glacial landforms and deposits are eroded and buried. In this paper, we present a new interpretation of buried, pre-Illinoian glacial features along the Laurentide glacial margin in northeastern Nebraska using Airborne ElectroMagnetics (AEM) supplemented with borehole logs and 2 m LiDAR elevation data. We detect and map large-scale (10^1 – 10^2 km) geological features using contrasts in electrical resistivity. The Laurentide glacial limit is marked by a continuous (>120 km) contrast between conductive ($<15 \Omega\text{-m}$), clayey tills and resistive ($>40 \Omega\text{-m}$) sandy sediments. Several smaller (10^2 km²) till salients extend 10s of km westward of this margin. We recognize a lithologically heterogeneous zone characterized by variable resistivity and complex geophysical structures extending as much as 17 km west of the glacial limit. This zone is interpreted as a glaciotectonic thrust complex, and it is analogous to a similar thrust complex in Denmark where structural analysis of co-located seismic and AEM surveys provides a standard for comparison. Our study suggests that the maximum advancement of pre-Illinoian glacial ice into Nebraska involved extensive deformation of sedimentary strata, local overriding of these deformed strata by smaller ice tongues, and emplacement of tills as much as 30 km west of the principal Laurentide ice margin. These insights provide the first glimpse of the large-scale stratigraphic architecture of glacial sediments in Nebraska and point to future clarifications of the geology and geomorphology of the Laurentide glacial limit.

1. Introduction

Glacial landforms constitute fundamental evidence of ancient glaciations and ice-marginal positions (Bickerdike et al., 2016; Chandler et al., 2018; Clark et al., 2004; Dyke and Prest, 1987; Kleman et al., 1997; Sollid and Sørbel, 1994). Constructional sediment-landform assemblages—such as till plains, push and hummocky moraines, outwash plains, proglacial fans, eskers, and kames—characterize the glacial margin environment (Bennett, 2001; Evans et al., 1999; Evans and Rea, 1999). Sediments deposited in this zone are distinctive and exhibit abrupt lateral facies changes indicative of large energy gradients

(Brodzikowski and van Loon, 1987). Geomorphic evidence of glacial margins during the Last Glacial Maximum, or LGM (26.5–19 ka)(Clark et al., 2009), is readily discernible in both landforms and sediments in the Northern Hemisphere (Antevs, 1929; Grosswald and Hughes, 2002; Margold et al., 2018; Prest et al., 1968), including the American Midwest (e.g. Syverson and Colgan, 2011). Middle Pleistocene (Illinoian) glacial landforms have also been described in that same part of the USA, although some of them are partially eroded or buried by loess (Leighton, 1959; Leighton and Brophy, 1961; Stiff and Hansel, 2004). In comparison, Early and early Middle Pleistocene (pre-Illinoian, or pre MIS-6) glacial landforms are sparse and subdued. Only the most pronounced

* Corresponding author.

E-mail addresses: jkorus3@unl.edu (J.T. Korus), rjoeckel3@unl.edu (R.M. Joeckel), jabraham@aquageoframeworks.com (J.D. Abraham), ahc@geus.dk (A.-S. Høyer), fjjoer@rm.dk (F. Jørgensen).

<https://doi.org/10.1016/j.qsa.2021.100026>

Received 19 February 2021; Accepted 26 March 2021

Available online 31 March 2021

2666-0334/© 2021 The Authors. Published by Elsevier Ltd. This is an open access article under the CC BY-NC-ND license (<http://creativecommons.org/licenses/by-nc-nd/4.0/>).

geomorphological characteristics of these older landforms are preserved on the modern land surface. Most of the evidence has been removed by younger glaciations, is concealed by erosional overprinting, or is buried.

There were multiple Pleistocene ice advances in the Northern Hemisphere prior to 0.6 Ma, including at least seven advances into midcontinental USA (Balco and Rovey, 2010; Balco et al., 2005; Barendregt and Duk-Rodkin, 2004; Batchelor et al., 2019; Ehlers and Gibbard, 2007; Haug et al., 2005). Pre-Illinoian tills have been recognized from approximately 97.5° in Nebraska to near 75° W in Pennsylvania (Balco and Rovey, 2010; Braun, 2004; Stiff and Hansel, 2004; Szabo and Chanda, 2004). Ice lobes have been proposed on the basis of modern drainage patterns and from the geographic distributions of certain erratics (Aber, 1999; Aber and Apolzer, 2004; Reed and Dreeszen, 1965; Wayne, 1985; Willard, 1980). Likewise, preglacial and pre-Illinoian ice-marginal streams have been inferred from maps of the buried bedrock surface and the distributions of coarse-grained fluvial deposits (Dreeszen and Burchett, 1971; Heim and Howe, 1963; Howe, 1968; Lugin, 1935; Todd, 1911; Witzke and Ludvigson, 1990). There is also sedimentary evidence for pre-Illinoian ice-marginal lakes (Ramage et al., 1998; Stanley, 1974) and glacial outburst channels (Bjornstad et al., 2001). Nevertheless, the positions of ice margins and the spatial distribution of ice-marginal landforms has remained mostly conjectural and key aspects of pre-Illinoian glaciations remain poorly understood.

Buried glacial landforms can be investigated by mapping the architecture of glacial deposits and erosional bedrock surfaces (Räsänen et al., 2009). Traditional sources of data, such as drill cuttings, cores, soil surveys, isolated outcrops, topographic maps, and land-based geophysics, supply most of the evidence for pre-Illinoian glaciations in the USA midcontinent (Aber, 1999; Aber and Apolzer, 2004; Jennings et al., 2013; Reed and Dreeszen, 1965; Roy et al., 2004; Soller, 1992; Wayne, 1985). But these methods are problematic for mapping heterogeneous and structurally complex strata because the sample density is often too sparse to resolve key aspects of geological variability. Geophysical methods offer a solution for mapping heterogeneous strata and buried landforms that have little to no topographic expression on the modern land surface (Jørgensen et al., 2003; Sharpe et al., 2003). Recent developments in airborne electromagnetics (AEM), in particular, have made it possible to rapidly map large areas at high lateral resolution for comparatively low cost (Auken et al., 2017; Robinson et al., 2008). AEM has been used to map complex subsurface geology, including buried valley networks (Høyer et al., 2015; Korus et al., 2017; Oldenborger et al., 2013) and glaciotectionic structures (Høyer et al., 2013; Jørgensen et al., 2012). A decade of AEM surveys in eastern Nebraska has emphasized regional

hydrogeologic mapping (Divine et al., 2009), but these surveys have also revealed details of Pleistocene stratigraphy over large areas of north-eastern Nebraska. Here, the Laurentide Ice Sheet advanced over preglacial and proglacial deposits, creating a complex arrangement of heterogeneous stratigraphic units that could not have been mapped from borehole data alone. Therefore, we utilize recent AEM data to map multiple glacial margin positions and a zone of buried glaciotectionic structures over an area of 6200 km², providing new insights into the extent and dynamics of the Laurentide ice sheet at its maximum extent during the Early to early Middle Pleistocene in midcontinental North America. Our study is the first major advance in understanding the large-scale (10¹–10³ km) architecture of glacial sediments in Nebraska in a century and a half of geologic research.

2. Geographic and geologic setting

A large region of Illinoian and pre-Illinoian glacial deposits exists south of the Wisconsinan ice limit in the central U.S.A. (Fig. 1). Pre-Illinoian glacial deposits are widespread and well-known in most of southern Iowa, northern Missouri, northeastern Kansas, and eastern Nebraska, to which Illinoian and Wisconsinan advances did not extend. Unlike other Midwestern states, there is no stable set of stratigraphic names for individual tills in Nebraska. Instead, letter designations have been applied to tills of different relative ages and magnetic polarities (Fig. 2). There were as many as seven advances of the Laurentide ice sheet in eastern Nebraska from ~2.5–0.6 Ma (Balco et al., 2005; Boellstorff, 1978a, b; Roy et al., 2004). The maximum number of tills visible in one place, however, ranges from 1 to 3 (Roy et al., 2004).

The Dissected Till Plains of eastern Nebraska is characterized by rolling hills, flat plains flanked by hilly, dissected uplands and valley side-slopes, and flat bottomlands along stream valleys (Fenneman, 1946; Korus et al., 2013; Luman et al., 2002; Prior, 1976). A series of parallel, semi-continuous, linear to broadly arcuate upland divides in glaciated eastern Nebraska (Fig. 3) have been interpreted by a few others as morainal ridges (Dreeszen, 1970; Reed and Dreeszen, 1965). Aber (1999) and Aber and Apolzer (2004) considered these ridges to be Laurentide ice-margin positions, but they conceded that an absence of constructional geomorphology hinders more specific genetic interpretations. In any event, the specific ages of the ridges are unknown.

Bedrock in the study area comprises both Cretaceous and Neogene strata (Fig. 2). Lithologically variable Cretaceous strata in the study area dip gently (~0.1°) to the west-northwest, whereas the erosion surface on the Cretaceous System slopes gently (<0.1°) to the east. In ascending

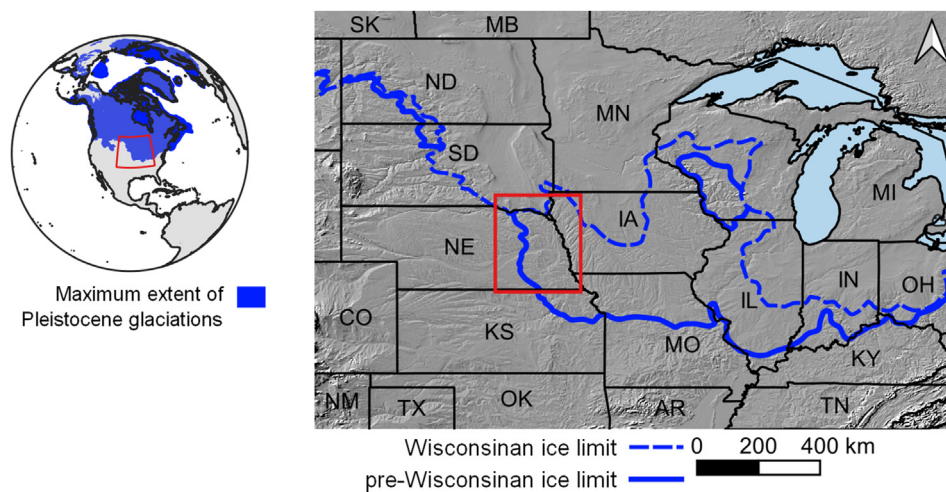


Fig. 1. Extent of Pleistocene glacial maximum in the northern hemisphere and map of the central and eastern U.S.A. showing approximate extent of pre-Wisconsinan and Wisconsinan glaciations. Red box, including eastern Nebraska (NE) and environs, shows extent of maps in Fig. 3. Abbreviations for state names are standard U.S. Postal Service usage.

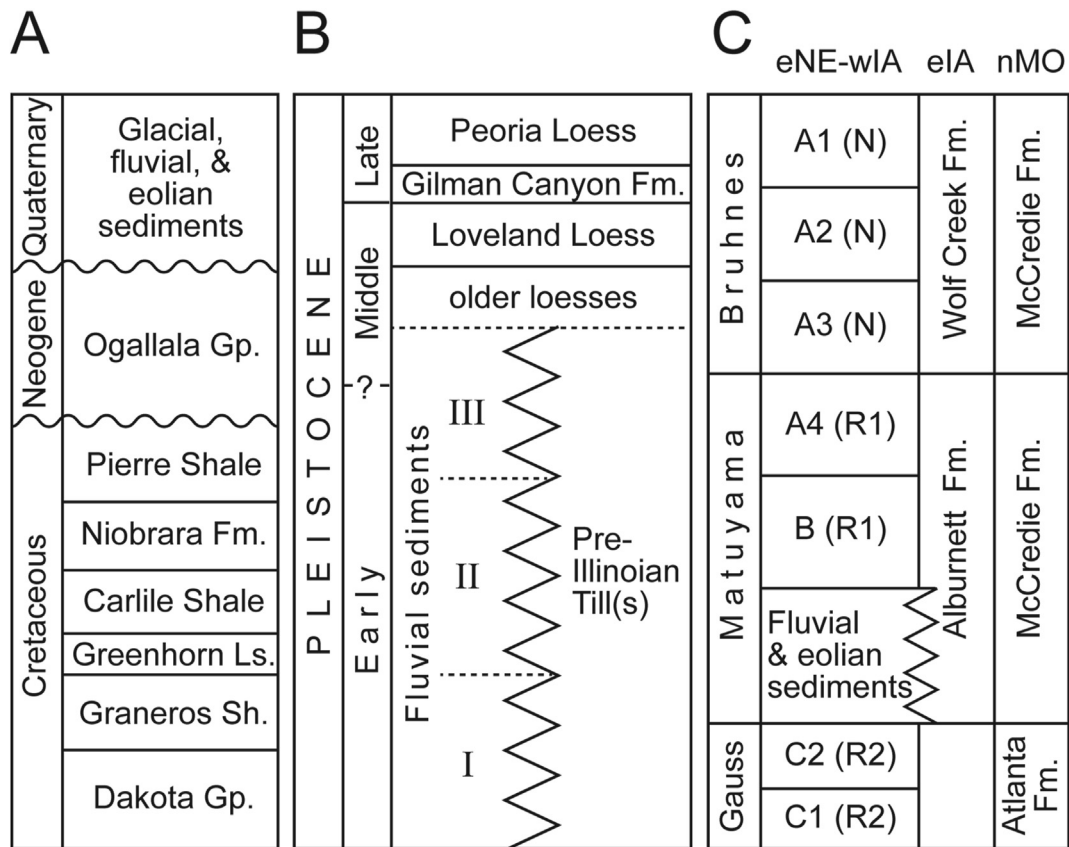


Fig. 2. Stratigraphic charts. A. Generalized bedrock stratigraphy of northeastern Nebraska. The unconformity atop the Cretaceous is regionally angular (bedrock strata dip $\sim 0.1^\circ$ west-northwest), such that the bedrock surface is composed of progressively older units to the east. B. Detailed stratigraphy of Pleistocene strata in the study area. Formal stratigraphic naming schemes have not been defined in the area. C. Stratigraphic correlation chart (including geomagnetic polarity timescale) for tills in eastern Nebraska (eNE), western Iowa (wIA), eastern Iowa (eIA), and northern Missouri (nMO), after Balco et al. (2005); Boellstorff (1978a, 1978b); Roy et al. (2004).

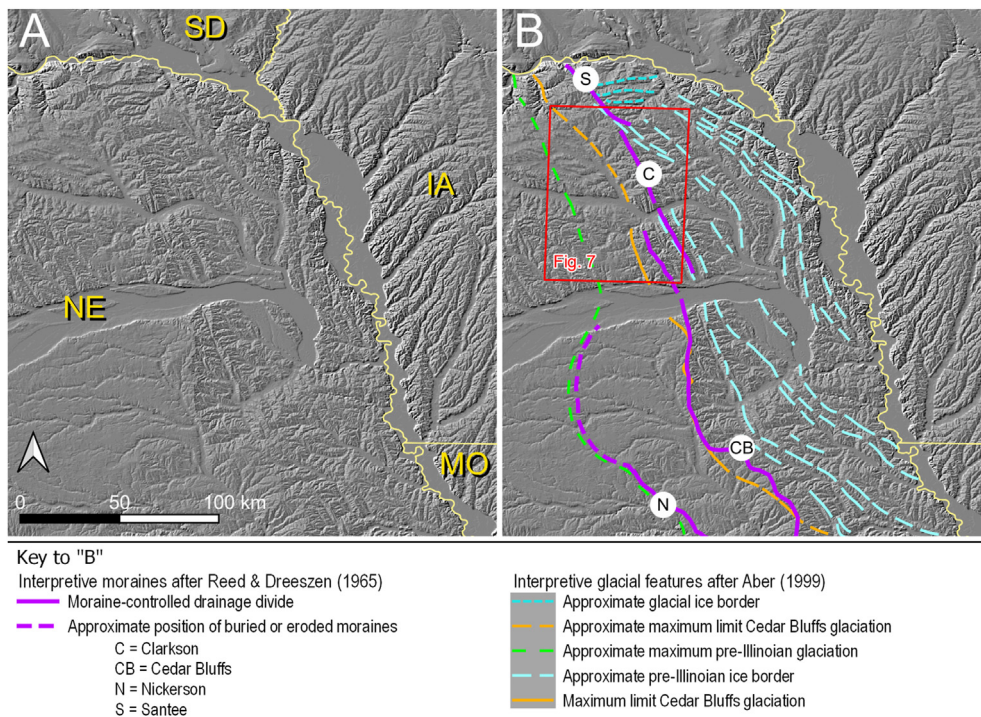


Fig. 3. Previously mapped glacial margin features in eastern Nebraska (NE) interpreted from topography and boreholes: map includes parts of adjacent South Dakota (SD), Iowa (IA), and Missouri (MO). A. Shaded relief map of eastern Nebraska and surrounding states. B. Interpreted glacial features from Aber and Apolzer (2004) and Reed and Dreeszen (1965). Purple lines are moraines interpreted by Reed and Dreeszen (1965): S = Santee, C = Clarkson, CB = Cedar Bluffs, N = Nickerson.

stratigraphic order, the Cretaceous succession is: (1) the Dakota Group (sandstones, siltstones, and shales), (2) Graneros Shale, (3) Greenhorn Limestone (chalky shales and chalky limestones), (4) Carlile Shale, (5) Niobrara Formation (chalky shale, chalky limestone, and argillaceous chalk) and (5) Pierre Shale. The Neogene Ogallala Group—consisting of semiconsolidated sandstones, siltstones, and claystones—is a fundamental part of the High Plains aquifer. It is present atop the Cretaceous in the northern part of the study area. The Ogallala Group extends across several Great Plains states, but its easternmost extent is in northeastern Nebraska: the only place where the High Plains aquifer abuts glacial deposits.

Glacial deposits rest unconformably atop bedrock or, locally, atop the fills of Pliocene to early Pleistocene paleovalleys incised into bedrock. Glacial sediments attain a total thickness of as much as 90 m (Dreeszen, 1970) and comprise matrix-rich, clayey tills and interspersed, sorted sands and gravels, as well as paleosols (Rovey and Bettis, 2014; Roy et al., 2004; Wayne, 1985). Outcrops of glacial sediment near the Laurentide glacial margin in eastern Nebraska are rare, particularly in the present study area, where no details of stratigraphic architecture can be ascertained from them. In northeastern Kansas, however, isolated outcrops have exposed small-scale structural deformation features (Aber, 1988, 1991; Aber et al., 1989; Dellwig and Baldwin, 1965; Dort Jr, 1987; Roy et al., 2004).

3. Materials and methods

Geophysical and geological data were assembled from multiple databases and integrated into a 3D virtual environment using the commercial software GeoScene3D. The depths of boreholes and geophysical inversion models were referenced to a digital elevation model generated from 2 m-resolution LiDAR. The coordinate system of all project data is Nebraska State Plane Meters (EPSG 32104).

3.1. Airborne Transient Electromagnetics (TEM)

Airborne Transient Electromagnetic (TEM) investigations provide characterization of subsurface electrical properties using electromagnetic induction (Christiansen et al., 2006). To collect TEM data, an electrical

current is sent through a transmitter (Tx) coil—a large loop of wire consisting of multiple turns—generating an electromagnetic (EM) field. After the EM field produced by the Tx coil is stable, it is switched off as abruptly as possible. The EM field dissipates and decays with time, traveling deeper and spreading wider into the subsurface (Fig. 4A). The rate of dissipation is dependent on the electrical properties of subsurface geologic materials. These properties, in turn, are determined by the amount of mineralogical clay, water content, ionic composition of pore water, metallic mineralization, and percentage of void space in the subsurface (Kirsch, 2006; Paine and Minty, 2005; Palacky, 1988). At the moment of turnoff, a secondary EM field is generated within the subsurface, and as it decays, it generates a current in a receiver (Rx) coil per Ampere's Law. This current is measured in several different time bands known as gates (Fig. 4B). Measurements of the induced current determine the time rate of decay of the magnetic field (dB/dt). When compiled in time, these measurements constitute a “sounding” at one location (Fig. 4C). The spacing between soundings depends on flight speed and measurement interval, but it is typically a few tens of meters. The sounding curves are numerically inverted to produce a model of subsurface resistivity as a function of depth (Fig. 4D). Inversion relates the measured geophysical data to probable physical earth properties.

TEM surveys in eastern Nebraska have been flown with the SkyTEM 508, 304M, and 312 systems, which are rigid frame, dual-magnetic moment (Low and High) TEM systems (SkyTEM, 2018; Sørensen and Auken, 2004). The systems vary in terms of the area of the Tx coil, number of turns of wire, and peak currents and magnetic moments for Low and High moments (Table 1). The 304M system is configured for greater sensitivity of near-surface layers compared to the 508 and 312 systems; however, the latter systems have greater depths of penetration. The systems utilize an offset Rx positioned slightly behind the Tx resulting in a ‘null’ position, which is where the intensity of the primary field from the system transmitter is minimized, increasing the receiver's sensitivity to the secondary fields. Each system is equipped with a Total Field magnetometer and data acquisition system, an AEM data acquisition system, two laser altimeters, two inclinometers, and three differential global positioning system (DGPS) receivers (two for the frame and one for the magnetometer).

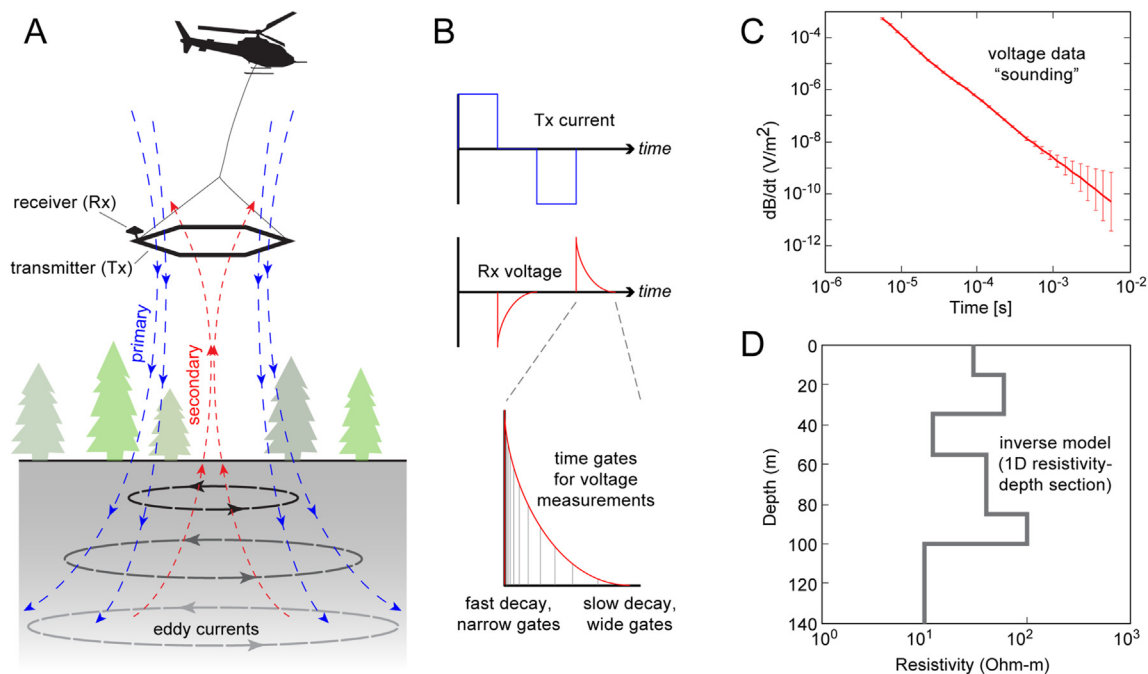


Fig. 4. Generalized description of SkyTEM system, measurements, and inversion model. A. Basic system geometry and electromagnetic field. B. Relationship between transmitter (Tx) and receiver (Rx) currents, as well as time gates within which voltage measurements are made. C. Example of a single sounding made from voltage measurements. D. 1D resistivity-depth model produced from numerical inversion of voltage sounding.

Table 1
Specifications of the SkyTEM instruments used in this study.

		SkyTEM 508	SkyTEM 304M	SkyTEM 312
Low moment	Area of Tx coil (m ²)	536	337	337
	Turns of wire	1	1	2
	Tx			
	Peak current (A)	8.6	9	6
	Peak magnetic moment (A*m ²)	4600	3000	4100
High moment	Turns of wire	8	4	12
	Peak current (A)	127	120	110
	Tx			
	Peak magnetic moment (A*m ²)	540,000	160,000	450,000
	Area of Rx coil (m ²)	105	105	105

3.2. Airborne TEM data acquisition and processing

Multiple airborne TEM surveys were completed in eastern Nebraska during 2014–2018 as part of a multi-agency collaboration known as Eastern Nebraska Water Resources Assessment (ENWRA), which includes six Natural Resources Districts, or NRDs (Fig. 5). A total of 23,370 line-km of data were acquired over eastern Nebraska using a combination of the three SkyTEM systems described above. Surveys were designed to address local groundwater management issues of the NRDs, so the SkyTEM system configuration, flight line spacing and orientation, and inversion parameters vary according to the objectives of each group of surveys (Table 2). The first surveys were flown with SkyTEM 508 system in a rectilinear grid pattern with ~4.8 km line spacing and as reconnaissance lines spaced ~32 km apart. Later, detailed surveys in grids with 0.25–4.8 km line spacing were flown with the SkyTEM 304M system, and more sparingly, the 312 system.

All AEM data were processed to remove electromagnetic coupling

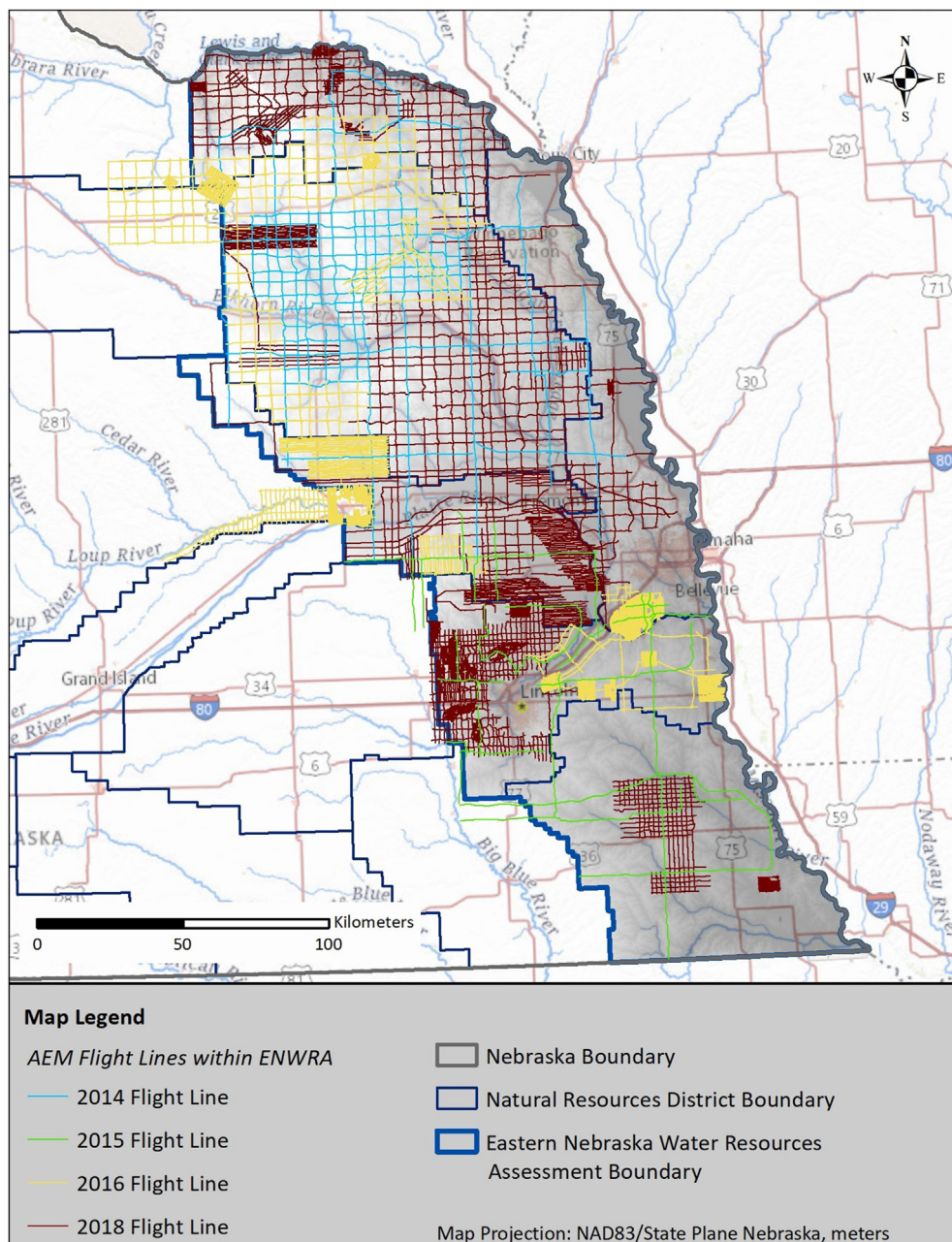


Fig. 5. Map of eastern Nebraska showing AEM flight lines grouped by year of acquisition.

Table 2
Details of AEM surveys and inversion models.

	LENRD 2014	ENWRA Phase 1 2014	ENWRA Phase 2 2015	ENWRA 2016	ENWRA 2018	LCNRD 2018
Acquisition dates	October 11–19, 2014	October 11–19, 2014	April 16–21, 2015	July 4 – August 3, 2016	June 13 – July 26, 2018	July 18–26, 2018
Acquisition length (km)	1471	889	550	9300	9829	1331
Approximate grid spacing (km)	4.8	32	32	variable (0.25–4.8)	variable (0.45–1.5)	4.8
SkyTEM system(s)	508	508	508	304M	304M	312
Inversion type	SCI (smooth)	SCI (smooth)	SCI (smooth)	SCI (smooth)	SCI (smooth)	SCI (smooth)
Spatial reference distance (m), power laws	100, 0.5	100, 0.5	100, 0.5	30, 0.5	30, 0.75	100, 0.75
Vertical constraints	2.0	2.0	2.0	2.7	2.4	2.4
Lateral constraints	1.3	1.3	1.3	1.6	1.4	1.4
Initial resistivity (ohm-m)	10	10	10	10	10	10
Workbench version	4.2.7.2	4.2.7.2	4.2.7.2	5.2.0.0	5.8.3.0	5.8.3.0
Number of inversion layers	30	30	30	30	40	40
Thickness of top layer (m)	5.0	5.0	5.0	3.0	1.0	3.0
Factor by which layer thickness increases	1.1	1.1	1.1	1.08	1.08	1.07
Thickness of bottom layer (m)	40.7	40.7	40.7	25.9	8.62	28.3
Depth of bottom layer (m)	500	500	500	311.8	324.9	548.9
References	Carney et al. (2015a)	Carney et al., (2015b), Carney et al., (2015c)	Carney et al., (2015b); Carney et al., (2015c)	AGF 2017a; AGF 2017b; AGF 2017c; AGF 2017d; AGF, 2017e; AGF, 2017f; AGF, 2017g; AGF, 2017h	AGF 2018; AGF 2019a; AGF 2019b; AGF 2019c; AGF 2019d; AGF 2019e	AGF (2019d)

(EM Coupling) impacts and other noise associated with aircraft movement and excessive ground clearance due to the flying over tall power lines. The AEM data were inverted with Aarhus Workbench software using the Spatially-Constrained Inversion (SCI) option (Viezzoli et al., 2008) and a smooth model with 30–40 layers, each with a starting resistivity of 10 Ω -m (equivalent to a 10 Ω -m half space). Inversion parameters and layer thicknesses varied according to available inversion codes appropriate to each system (Table 2). The thickness of the layers increases with depth because the resolution of the induction technique decreases with depth.

3.3. Borehole data

We used borehole data from water wells registered at the Nebraska Department of Natural Resources (NDNR) and from geologic test holes drilled by the Conservation and Survey Division (CSD). The DNR well registrations contain descriptions of cuttings collected during the drilling of water wells. Most of these descriptions were made by water-well contractors with cursory training in the description of cuttings. These data vary in quality and reliability, and the lithological descriptions are not assigned to formal stratigraphic units. These descriptions still have value when they are interpreted in the context of CSD test holes, which were drilled as part of a statewide geological investigation program and were planned, described, and archived by professional geologists. Most CSD test holes were drilled with mud rotary techniques and logged with wireline geophysical instruments. Only a few cores were drilled in certain locations. Although there are many fewer CSD test-hole logs than DNR well logs, their quality and reliability is much greater. Furthermore, the CSD database contains records of the stratigraphic units encountered in each test hole.

3.4. Interpretation of resistivity-depth profiles

An understanding of the principal controls on subsurface electrical properties in the region of interest is a prerequisite to interpreting

geophysical images (Knight and Endres, 2005). In areas of eastern Nebraska without saline porewater, which includes the present study area, previous research has established that the volume of mineralogical clay in the subsurface is the chief control on resistivity of unconsolidated materials above bedrock (Carney et al., 2015a; Korus, 2018; Korus et al., 2017). This relationship is consistent with findings in other places with similar geology, such as Denmark (Barfod et al., 2016) and Manitoba (Oldenborger et al., 2013). Tills in eastern Nebraska are rich in clay (Rovey and Bettis, 2014; Roy et al., 2004; Wayne, 1985) and thus, have relatively low electrical resistivity (<20 Ω -m). Clay-poor silts, sands, and gravels, in comparison, have relatively high electrical resistivity (>50 Ω -m). Mixed lithologies of clay and sand have resistivity values ranging from ~20 to 50 Ω -m. Comparisons of co-located borehole lithology, borehole resistivity, and AEM resistivity data for a geological test hole in the study area confirms this relationship (Fig. 6). We continually compared resistivity values to the logs of nearby boreholes to verify the resistivity-lithology relationship, finding it consistent throughout the study area. Thus, we used contrasts in resistivity to identify geological interfaces (e.g. bedding contacts, faults, unconformities) and correlate them along and between profiles, starting in areas of high-density AEM data (200–300 m spacing between flight lines) and then extending into areas of low-density AEM data (~5 km spacing between flight lines). The positions of the features of interest were digitized in the profiles and 3D views, and then we used GIS to produce maps showing the extents of subsurface features.

4. Results

We recognize two types of large-scale (10^1 – 10^2 km) features—till margins and a heterogeneous zone—near the glacial margin in the study area (Fig. 7). Other, smaller features can be identified locally in the AEM profiles. Nevertheless, we focus on the geophysical and geological characteristics of features relevant to mapping the glacial margin.

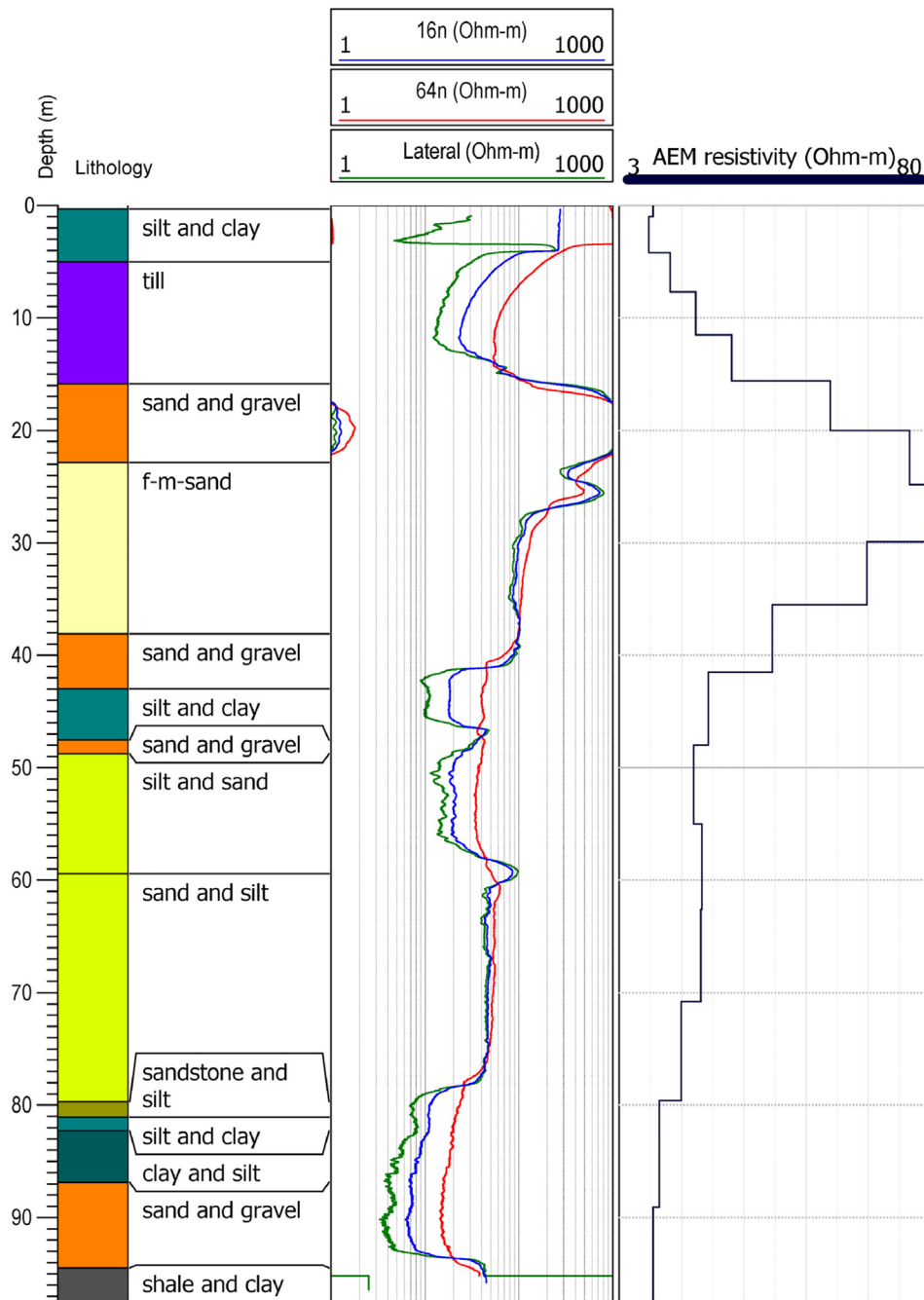


Fig. 6. Borehole lithology and geophysical resistivity log of a geologic test hole drilled by the Conservation and Survey Division (CSD), compared with co-located AEM resistivity-depth model.

4.1. Till margins

Till margins are marked by a dramatic contrast in resistivity across the previously mapped Laurentide glacial limit. This contrast is between the generally conductive (<15 Ω-m), thick (>40 m), clay-rich diamicton (till) in the eastern part of the study area and the laterally equivalent, but comparatively resistive (>40 Ω-m) sand, gravel, and silt (including comparatively thin, clayey diamicton) in the western part of the study area (Fig. 8). These two lithofacies are separated by an abrupt resistivity contrast (~25 Ω-m/10 m) defining an eastward-dipping (<5°) surface with vertical relief of as much as 60 m (Fig. 8). In most places, this surface is listric at depth, becoming horizontal and merging with the bedrock surface. It is not possible to determine whether one or more tills are present east of the resistivity contrast. Nevertheless, this distinctive

interface defines the boundary of widespread, continuous till in the study area, and so its western boundary is referred hereafter as the principal till margin (PTM). The PTM is mapped as a generally straight, NNW-SSE line 120 km in length (Fig. 7).

In some areas, the till lithofacies overlaps the sand lithofacies west of the PTM, resulting in a configuration of thin (<40 m) till sheets that protrude slightly westward (Fig. 9). These thin till sheets form three distinct “salients” or lobate extensions in map view (Fig. 7). The westernmost till salient (2 in Fig. 7) extends at least 18 km west of the PTM, and the till salient in the southern part of the study area (3 in Fig. 7) extends 30 km west. The PTM can be traced westward within profiles as a horizontal to gently (<1°) west-dipping surface. The surface rises abruptly, forming additional east-dipping till margins (Figs. 9–10). These multiple till margins exist at successively higher elevations westward

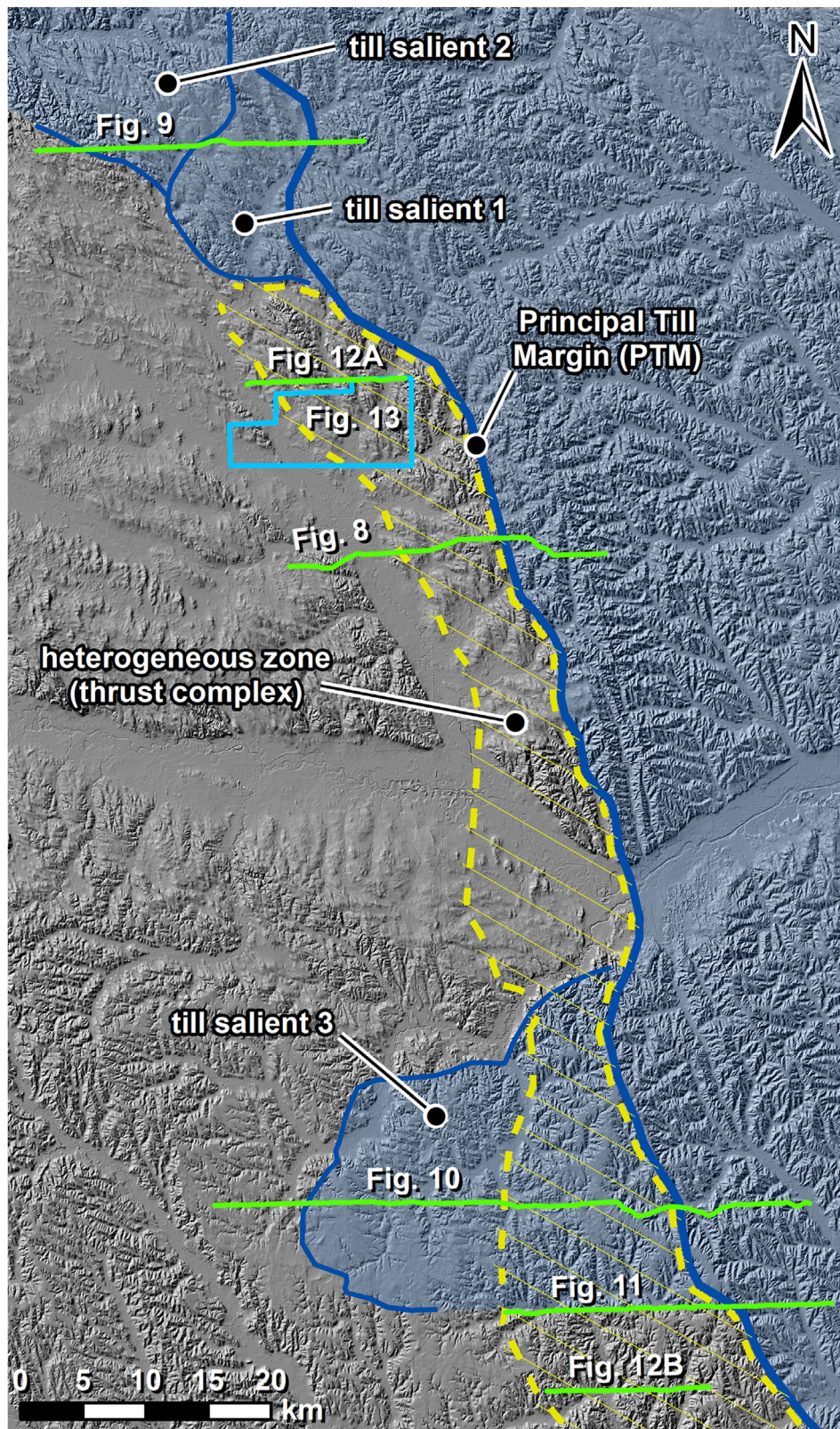


Fig. 7. Map of study area showing locations of profiles (green lines) shown in this paper and boundaries of interpretive glacial margin features.

such that the thickness of the sand lithofacies increases at the expense of the till lithofacies (Fig. 9). Isolated, high-resistivity sand bodies exist within and above the westward-protruding till salients (i.e. “buried valley” in Fig. 10). The till salients do not correspond directly to any modern landforms.

4.2. Heterogeneous zone

There is a zone of heterogeneous resistivity and highly variable lithology extending westward 6–17 km from the PTM (Fig. 7). This zone comprises vertically and horizontally discontinuous resistivity structures

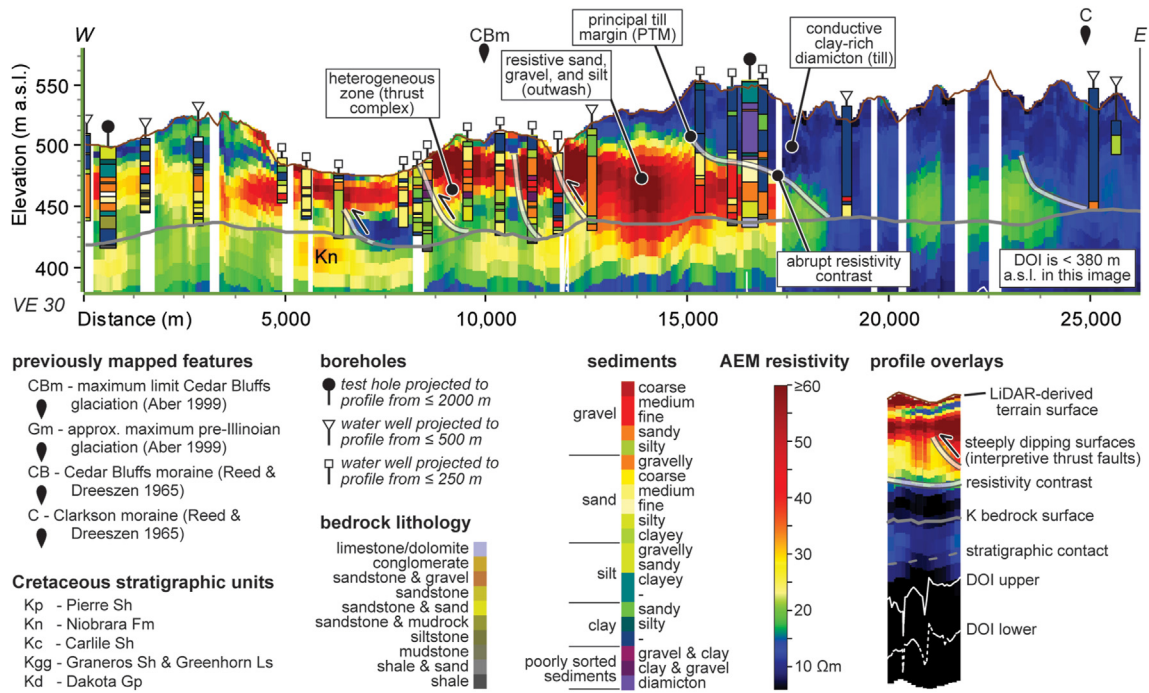


Fig. 8. Profile showing boreholes, interpretive geological features, and portion of AEM profile along flight line 100701 from 2014 SkyTEM 508 survey. See Fig. 7 for location.

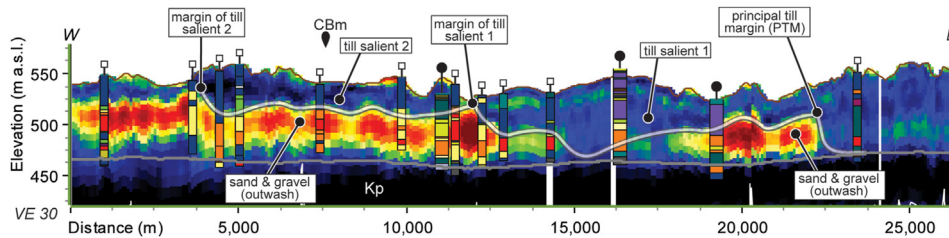


Fig. 9. Profile showing boreholes, interpretive geological features, and portion of AEM profile along flight line 124900 from 2016 SkyTEM 304M survey. See Fig. 7 for location and Fig. 8 for legend.

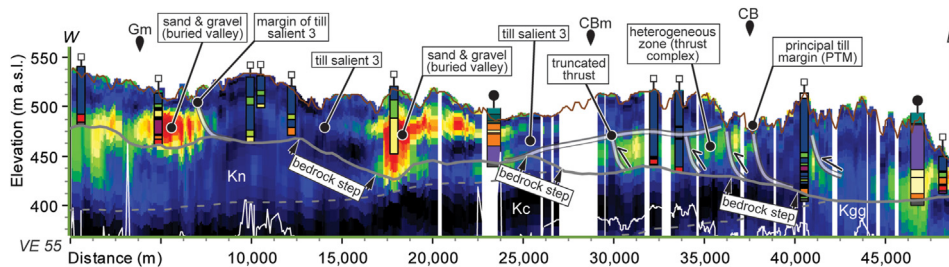


Fig. 10. Profile showing boreholes, interpretive geological features, and portions of AEM profile along flight lines 121301 from 2016 SkyTEM 304M survey and 908300 from 2018 SkyTEM 304M survey. See Fig. 7 for location and Fig. 8 for legend.

that are difficult or impossible to correlate between widely spaced (>1 km) AEM profiles. These structures consist of high-resistivity sand and gravel bodies (~0.5–2 km wide, 20–50 m thick) separated by thin (10–30 m) layers of low-resistivity, clay-rich sediments (including possible tills), and they appear to be tilted upward in imbricate stacks separated by steep (10–20°), eastward-dipping surfaces (Figs. 10–12). The upper parts of these structures are commonly truncated along a horizontal or a shallow-dipping (<1°) surface (Figs. 10 and 11). In these cases, till salients overlie the heterogeneous zone and the imbricate structures are truncated at the base of the till sheet (Figs. 10 and 11). In

other areas, the structures are truncated by the present land surface (Fig. 12A) or beneath the thin loess cover (Fig. 12B). The base of the heterogeneous zone generally corresponds to the bedrock surface, but in some profiles, it rises atop a gently sloping (<1°), eastward-dipping surface (Fig. 11) that downlaps onto and merges with the bedrock surface eastward. The bedrock surface may exhibit a relatively abrupt change in elevation (20–30 m over distances of ~1–5 km), or “step”, at the location of convergence (Figs. 10–12). At its western edge, the lower surface of the heterogeneous zone is horizontal and lies ~20–30 m above the bedrock surface (Fig. 12A).

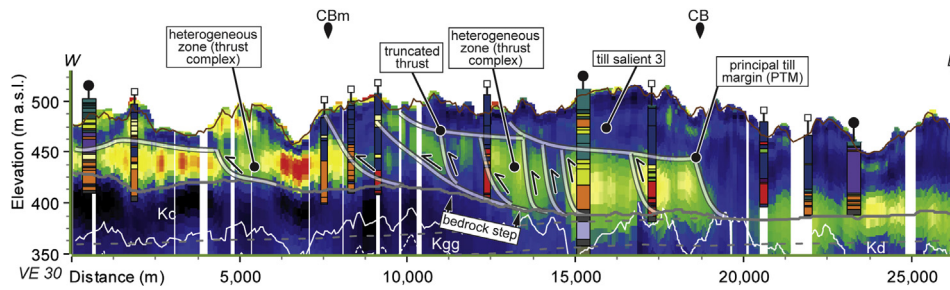


Fig. 11. Profile showing boreholes, interpretive geological features, and portions of AEM profile along flight lines 110901 from 2016 SkyTEM 304M survey and 908700 from 2018 SkyTEM 304M survey. See Fig. 7 for location and Fig. 8 for legend.

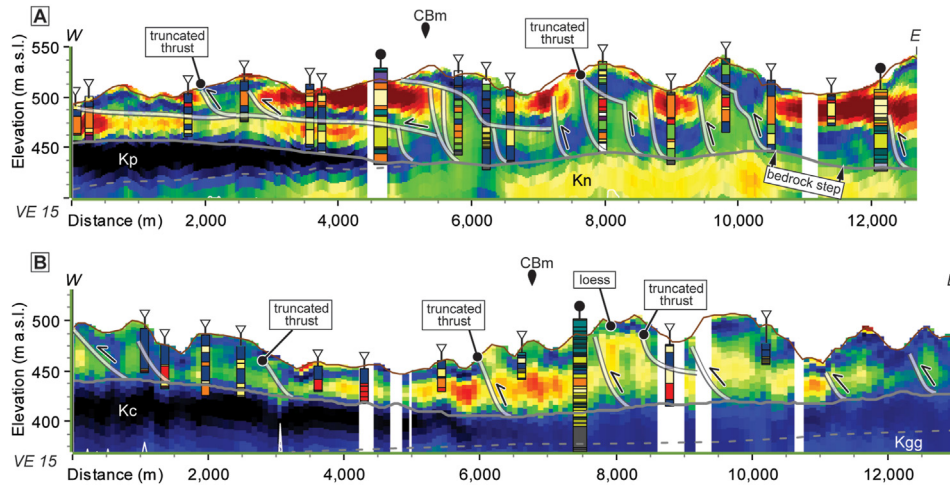


Fig. 12. Interpretive thrust complexes. A. Profile showing boreholes, interpretive geological features, and portion of AEM profile along flight line 904301 from 2018 SkyTEM 304M survey. B. Profile showing boreholes, interpretive geological features, and portion of AEM profile along flight line 112901 from 2016 SkyTEM 304M survey. See Fig. 7 for location and Fig. 8 for legend.

In areas of closely spaced (~0.25 km) flight lines, 3D grids of AEM resistivity reveal the shape and continuity of the structures (Fig. 13). Near the land surface (0 – 3 m in depth) there is a repeating, heterogeneous pattern of alternating low- and high-resistivity units. Each of these units is ~1–2 km wide in the E-W direction and ~3–4 km long in the N-S direction. Conductive bodies in this zone generally correspond to ridges between small stream valleys. Resistive bodies generally outcrop on the west-facing sides of valleys and are continuous beneath the valley bottoms.

Individual subsurface structures are, in most cases, difficult to correlate between widely spaced profiles. Nevertheless, it is possible to map the heterogeneous zone continuously (except where it is eroded in a river valley) for ~100 km from the southern border of the study area to the location of the till salient in the north (Fig. 7). The eastern boundary of the heterogeneous zone is uniformly prominent because it is well-defined by the PTM (1 in Fig. 7). The western boundary of the zone is inconspicuous because its constituent structures gradually give way to laterally continuous, horizontally stratified resistivity bodies (Fig. 12A).

Individual subsurface structures are, in most cases, difficult to

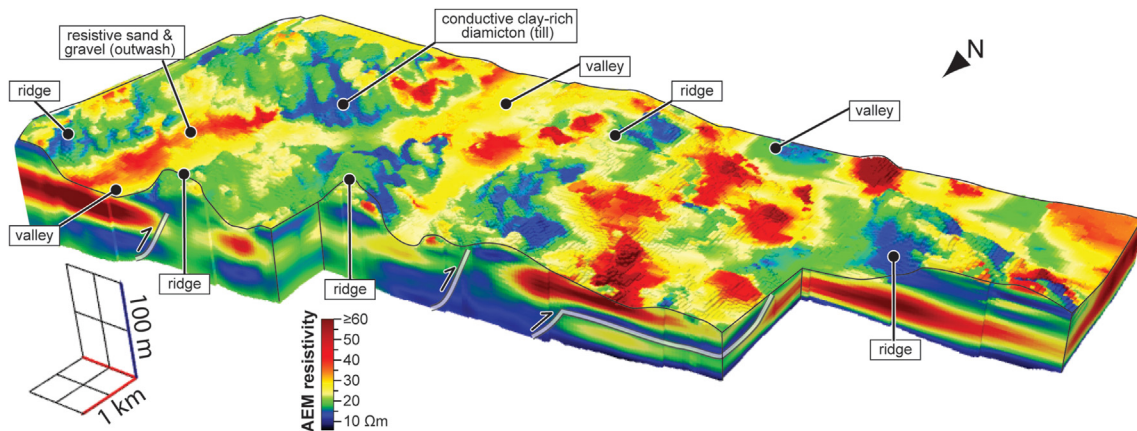


Fig. 13. Block model of AEM resistivity in thrust complex. Vertical exaggeration = 15. See Fig. 7 for location.

5. Discussion

5.1. Interpretation of ice-marginal features

We interpret the PTM as the terminal position of the main body of the Laurentide ice sheet during its maximum pre-Illinoian extent. Thick successions of clayey till to the east were deposited primarily in the glacial environment where a continuous ice sheet existed during one or more glacial advances. The stratified, high-resistivity ($>20 \Omega\text{-m}$) deposits lying west of the PTM formed in terminal and proglacial environments, where multiple depositional and deformational processes give rise to heterogeneous assemblages of coarse and fine sediments (Brodzikowski and van Loon, 1987). Although the interpretive ice margin does not precisely correspond to any particular landforms, it roughly parallels the ‘moraine ridges’ described by Dreeszen (1970) and Reed and Dreeszen (1965)—and particularly the so-called Cedar Bluffs “moraine.” We refrain from using the term “moraine”, however, because the Laurentide ice margin we describe is not defined by a constructional landform. Nevertheless, it is common for moraines to consist chiefly of diamicton (Johnson and Menzies, 2002). Moreover, the series of ridges and drainage divides in the vicinity of the Laurentide ice margin, although heavily modified by post-depositional erosion, is likely a composite depositional fabric developed by multiple glacial advancements into the same area.

High-resistivity ($>40 \Omega\text{-m}$) sand and gravel bodies 20–50 m thick and 3–15 km wide from east to west are common along the proposed ice margin. These sediment bodies are elongate and oriented parallel to the ice margin, and they also thin and fine away from the margin, hence becoming less resistive westward (Figs. 8 and 9). These characteristics are consistent with an interpretation as proglacial outwash fans or ice-marginal meltwater stream deposits (Brodzikowski and van Loon, 1987; Eyles and Eyles, 2010). Following Korus et al. (2017), we also interpret isolated sand lenses as the buried valleys of glacial meltwater streams (Fig. 10). The till salients are interpreted as smaller ice margins formed by local ice-lobe advances, possibly due to glacial surges (e.g. Evans and Rea, 1999; Ingólfsson et al., 2016). The ice overrode the proglacial sandy lithofacies and emplaced—either by subglacial till deposition or glaciotectionics—sheets of till extending as much as 30 km from the PTM.

We interpret the zone of heterogeneous resistivity and lithology as a glaciotectionic thrust complex. This complex contains imbricate thrust stacks, and folded, faulted, and truncated strata, forming a complex zone of heterogeneous geology. The abrupt eastern boundary, eastward-dipping thrust planes, and the gradual decrease in complexity westward suggests that the principal stress direction imposed by advancing glacial ice was from the east to east/northeast. Some of the imbricate thrust planes originate from a gently inclined ($<1^\circ$) surface ramping upward some 100 m from the bedrock surface (Fig. 11). This geometry suggests that the ramped surface is a basal décollement. The décollement is rooted in the base of the Quaternary succession, or in some places, at the location of a “step” in the bedrock surface. The bedrock steps are linked to bedrock lows on the up-glacier side of the thrust.

5.2. Comparison to glaciotectionic complexes in Denmark

We compare our AEM interpretations in Nebraska to those made in geologically similar settings in Denmark. Danish AEM surveys were complemented by high-resolution seismic surveys, making them a standard for comparison (Høyer et al., 2013). Glaciotectionic structures are common in Denmark, which experienced several ice advances. Some of these structures can be observed directly in coastal outcrops (e.g. Klint and Pedersen, 1995; Pedersen, 1996; Pedersen, 2005) but they can also be recognized in seismic (e.g. Andersen, 2004) and electromagnetic images (Jørgensen et al., 2012). Furthermore, AEM data acquired over much of Denmark has revealed complex glacial stratigraphy and structures.

The Ølgod area in western Denmark lies near the western limit of the Saalian Warthe glacial advance. Complex glaciotectionic structures have been mapped there using multiple methods (Høyer et al., 2011, 2013), including AEM, high-resolution reflection seismic and borehole information including a deep investigation borehole with palynological analyses. These features include a sealed, large-scale cupola-hill-type glaciotectionic complex deeply rooted in a two-phase thrust-fault complex (Høyer et al., 2013). It formed during the Saalian glaciation and was truncated by subglacial erosion. A gridded 3D resistivity cube produced from the AEM data facilitated the construction of geologic cross sections.

The glaciotectionic complex could be discerned in both AEM and seismic sets from Ølgod, although in different ways (Fig. 14). The complex includes electrically conductive clay layers and resistive sand layers, providing a resistivity contrast that permits the mapping of structural features. Due to limitations in the resolution of AEM, only the larger folds and thrust structures were visible. Nevertheless, the dense data coverage and 3D grid allowed the structures to be mapped in three dimensions. A random cross section through the 3D resistivity grid shows a high degree of complexity with interspersed low resistivities ($<20 \Omega\text{-m}$) representing meltwater clay and Miocene clay and medium to high resistivities (50–100 $\Omega\text{-m}$) representing sandy Miocene and glacial sediments. The interpretations of folds and thrust faults is based on analysis of the 3D volume where neighboring data are included, thus providing clearer evidence of the presence of the structures (Høyer et al., 2013). The interpretations are also guided by relatively dense borehole information, which show Miocene and Eocene sediments atop Quaternary sediments in some locations (Fig. 14b). The root of the complex is at a depth of 180 m. The wavelength of the structures is approximately 300–700 m.

High-resolution seismic provided 2D structural information, which was compared with AEM from the 3D cube (Fig. 14b). The seismic reflections on the left side of the profile are rather chaotic and difficult to interpret, likely because of high complexity in the thrust fault complex. Thrust planes on the right half of the profile are recognized by displacement of the otherwise clear and coherent reflections. The displacement is not revealed by the AEM data, probably due to the lack of distinct resistivity contrasts among the layers in the dissected succession. The root of the thrust faults is difficult to decipher but it is likely deeper than 150 m. A previously published seismic section (Fig. 7 in Høyer et al., 2013) provides a clear picture of the glaciotectionic setting, including hanging-wall ramps and anticlines, detachment surfaces and folded sediments, and a thin-skinned thrust fault complex composed of primarily Miocene deposits deformed to depths of 160 m.

AEM data from Ølgod is a useful analog for interpreting glaciotectionic deformation in Nebraska. AEM surveys have significantly lower resolution than seismic surveys, but they still capture such complexes in 3D, reveal the orientations and lateral extents of structures, and provide information about the sedimentary properties of the complex.

5.3. Dynamic and stratigraphic considerations

Thrust complexes arise by two mechanisms: (1) the “pushing” of sediments in front of the ice margin (proglacial thrusting), and (2) thrusting within the glacial ice itself, which, upon melt-out, forms stacked sediment masses (englacial thrusting) (Bennett, 2001). The abrupt lateral change from clayey tills to sandy deposits at the PTM in our study area is compatible with deformation driven principally by the proglacial thrusting of a glaciofluvial sediment wedge formed in front of the Laurentide ice sheet. Thus, the abrupt resistivity contrast indeed delineates an ice margin. Englacial thrusting cannot be dismissed as a mechanism of deformation in the glaciotectionic zone because the relationship between thrust complexes and the ice margin is commonly indistinct (Aber et al., 1989; Bennett, 2001). Because tills can originate from the ablation of debris-rich ice masses, it seems likely that englacial thrusting would result in stacked, alternating masses of till and sand, forming an indistinct margin, not a sharp margin like we have documented here.

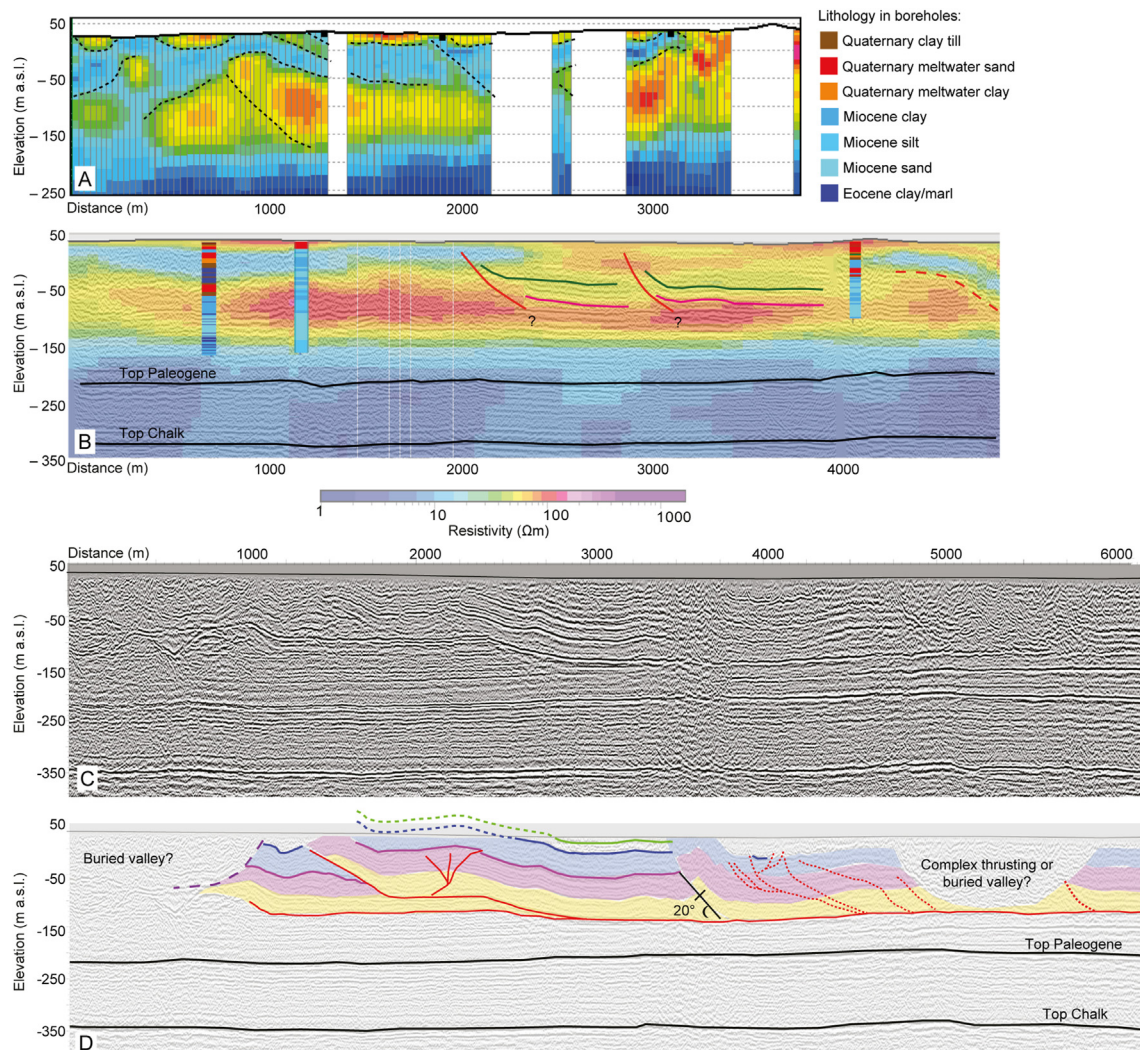


Fig. 14. A glaciotectionic complex in Denmark. A. Profile through a 3D resistivity grid. B. AEM superimposed on a co-located seismic line. Interpretive structural features are shown as dotted and solid lines. C. High-resolution seismic profile. D. Interpretation of seismic profile in C. After Hoyer et al. (2013).

Regardless of the mechanism of thrust emplacement, it is clear that advancements of smaller ice tongues (till salients) in our study area post-date the main phase of thrust development at the ice margin. Imbricated, thrust-faulted sediment bodies are undoubtedly truncated at the base of the overriding till sheets (Figs. 10 and 11). This relationship suggests that, where overridden, the proglacial thrust complex was subglacially modified in a subsequent ice advance. This scenario, which is typical of glacial margin environments, frequently produces cupola-hills, which are irregular hills with dome-like morphology and truncated internal structures (Aber et al., 1989). Nevertheless, any such landforms in the present study area are now buried by till and loess.

Bedrock lows up-glacier of steps in the bedrock surface (Figs. 10–12) present an interesting interpretational problem. If these steps were caused by thrust displacement of bedrock masses, then the upthrust bedrock would be present as allochthonous masses atop younger strata. Nevertheless, we have not identified any upthrust or displaced bedrock masses in the glaciotectionic complex. It is entirely possible that hypothetical upthrust bedrock masses would be indistinguishable in rotary boreholes, and there are exceedingly few cores of surficial sediment in the study area. Moreover, in the absence of prior accounts of glaciotectionic deformation in Nebraska, geologists and drillers have labored under the assumption that bedrock strata are everywhere undeformed, leading to possible dismissal of thrust bedrock by the interpreter and final description of them as layers of hard sediment. Finally, it is possible

that the basal décollement soles out at the bedrock surface, that there is no displacement of bedrock, and that the steps are buried, preglacial relief features such as cuestas. Because the ice advanced toward a reverse slope, such features would have promoted compressional deformation of the proglacial sediment mass at it was being squeezed between the ice and the bedrock barrier (Bennett, 2001). It is suggested that future investigations, including the drilling of intact cores, be conducted in the glaciotectionic zone to examine these possibilities in more detail.

One of the biggest challenges to studying the pre-Illinoian record is understanding the chronology of glaciation based on subsurface data. In the central U.S., such studies are often conducted by mapping and dating multiple tills in cores and widely scattered exposures (e.g. Boellstorff, 1978a; Roy et al., 2004). Because of the newly presented evidence for glaciotectionic deformation, which includes large-scale thrusting with décollement surfaces seated as much as 150 m below ground level, it is now evident that several stratigraphic considerations must be taken into account: inversion, repetition, thickening, and missing strata are potential complications in the analysis of till chronology near the glacial margin.

6. Conclusions

1. Airborne ElectroMagnetic (AEM) surveys permit the mapping of pre-Illinoian ice-margin features and glaciotectionic structures at the

Laurentide glacial margin in Nebraska. Our interpretation of these features is facilitated through comparisons to AEM surveys in geologically-similar Denmark, where seismic sections have augmented the interpretation of AEM. The glaciotectionic complexes in Denmark and Nebraska are strikingly similar. There are clear parallels terms of scale and complexity. Heterogeneous resistivity patterns, alternating resistive and conductive bodies, and inclined layers provide evidence of extensive glaciotectionic deformation.

2. The newly mapped principal till margin in this paper marks an abrupt juxtaposition of resistivity and lithology and corresponds roughly to the limit of the advance associated with the so-called Cedar Bluffs till (Dreeszen, 1970; Reed and Dreeszen, 1965; Swinehart et al., 1994). We interpret this feature as the main Laurentide ice margin. We also show that smaller till salients extend as far west as the pre-Illinoian glacial limit mapped by previous authors. Thus, the maximum extent of pre-Illinoian glaciation may actually reflect a series of smaller (10^2 km^2), irregularly spaced ice tongues that protruded ~20–30 km west from the Laurentide ice margin, rather than a single, continuous ice front.
3. The 10 km-wide, 100 km-long glaciotectionic complex that we identify is the first to be described in Nebraska. This complex appears in AEM as a zone of heterogeneous resistivity some ~100 m thick, between the bedrock surface and overlying till, loess, or the land surface. It includes imbricated thrust stacks and one or more décollement surfaces, sometimes coincident with stepped bedrock surfaces. Displaced bedrock masses cannot be identified, however, suggesting that the bedrock steps were pre-existing features that promoted compressional push-thrusting of unconsolidated sediments above them.
4. Future conceptualizations of the extent of pre-Illinoian glaciation in North America must consider that complex ice-margin environments probably existed then as in Wisconsinian times and around extant glaciers today. Maps of the ice margin must account for the possibility of glaciotectionic deformation and glacial surges extending 10's of km beyond the ice margin. Furthermore, stratigraphic inversion, repetition, thickening, or the removal of strata by glaciotectionic deformation are all complicating possibilities worthy of consideration.
5. Our interpretation of the Laurentide glacial margin provides a new model for the genesis of aquifers and confining units in northeastern Nebraska. This conceptualization provides a robust means of predicting the heterogeneity, continuity, and interconnectedness of aquifers. Such information is critical to managing water resources, remediating contaminated groundwater, designing aquifer recharge systems, and developing water supplies.

Data availability

Data used in this research are available from the Conservation and Survey Division (CSD), Institute of Agriculture and Natural Resources, University of Nebraska-Lincoln. The Nebraska GeoCloud (<https://go.unl.edu/geocloud>), which is managed by the CSD, is an online repository for Airborne ElectroMagnetic (AEM) and borehole data. AEM data are also available via the Eastern Nebraska Water Resources Assessment (ENWRA; <http://enwra.org/>). Borehole data can also be download or viewed in an interactive map via the CSD website (<http://snr.unl.edu/csd/>).

Declaration of competing interest

The authors declare that they have no known competing financial interests or personal relationships that could have appeared to influence the work reported in this paper.

Acknowledgments

This work was supported by Nebraska's Natural Resources Districts,

the Nebraska Environmental Trust, the Nebraska Natural Resources Commission (Water Sustainability Fund), Daugherty Water for Food Global Institute at the University of Nebraska, and the United States Department of Agriculture National Institute of Food and Agriculture, Hatch project NEB-21-177 (accession number 1015698) to J. Korus.

References

- Aber, J.S., 1988. West Atchison drift section. In: Hayward, O.T. (Ed.), South-Central Section of the Geological Society of America. Geological Society of America, Boulder, CO, pp. 5–10.
- Aber, J.S., 1991. The glaciation of northeastern Kansas. *Boreas* 20, 297–314. <https://doi.org/10.1111/j.1502-3885.1991.tb00282.x>.
- Aber, J.S., 1999. Pre-Illinoian glacial geomorphology and dynamics in the central United States, west of the Mississippi. In: Mickelson, D.M., Attig, J.W. (Eds.), *Glacial Processes Past and Present*. Geological Society of America, pp. 113–119.
- Aber, J.S., Apolzer, K., 2004. Pre-Wisconsinian glacial database and ice limits in the central United States. In: Ehlers, J., Gibbard, P.L. (Eds.), *Quaternary Glaciations: Extent and Chronology. Part II: North America*. Elsevier, pp. 83–88.
- Aber, J.S., Croot, D.G., Fenton, M.M., 1989. *Glaciotectionic Landforms and Structures*. Kluwer Academic Publishers, Dordrecht, The Netherlands.
- AGF, 2017a. Hydrogeologic Framework of Selected Area in Lower Loup Natural Resources District, Nebraska. Aqua Geo Frameworks, LLC, Mitchell, NE.
- AGF, 2017b. Hydrogeologic Framework of Selected Area in Twin Platte and Central Platte Natural Resources District. Aqua Geo Frameworks, LLC, Mitchell, NE.
- AGF, 2017c. Hydrogeologic Framework of Selected Areas in Lewis & Clark Natural Resources District, Nebraska. Aqua Geo Frameworks, LLC, Mitchell, NE.
- AGF, 2017d. Hydrogeologic Framework of Selected Areas in Lower Platte North Natural Resources District, Nebraska. Aqua Geo Frameworks, LLC, Mitchell, NE.
- AGF, 2017e. Hydrogeologic Framework of Selected Areas in Lower Platte South Natural Resources District, Nebraska. Aqua Geo Frameworks, LLC, Mitchell, NE.
- AGF, 2017f. Hydrogeologic Framework of Selected Areas in Sarpy County, Nebraska, Prepared for the Papio-Missouri River Natural Resources District. Aqua Geo Frameworks, LLC, Mitchell, NE.
- AGF, 2017g. Hydrogeologic Framework of Selected Areas in the Lower Elkhorn Natural Resources District, Nebraska. Aqua Geo Frameworks, LLC, Mitchell, NE, p. 109.
- AGF, 2017h. Mapping the Hydrogeology of the Bazile Groundwater Management Area with Airborne Electromagnetics Surveys, Prepared for Bazile Groundwater Management Area Project (Lewis and Clark Natural Resources District, Lower Elkhorn Natural Resources District, Lower Niobrara Natural Resources District, and Upper Elkhorn Natural Resources District). Aqua Geo Frameworks, LLC, Mitchell, NE.
- AGF, 2018. Airborne Electromagnetic Mapping and Hydrogeologic Framework of Selected Regions of the Eastern Nebraska Water Resources Assessment Area: Chapter on the Lower Elkhorn Natural Resources District, Revision 1. Aqua Geo Frameworks, LLC, Mitchell, NE.
- AGF, 2019a. Airborne Electromagnetic Mapping and Hydrogeologic Framework of Selected Regions of the Eastern Nebraska Water Resources Assessment Area: Chapter on the Lewis and Clark Natural Resources District. Aqua Geo Frameworks, LLC, Mitchell, NE.
- AGF, 2019b. Airborne Electromagnetic Mapping and Hydrogeologic Framework of Selected Regions of the Eastern Nebraska Water Resources Assessment Area: Chapter on the Lower Platte North Natural Resources District. Aqua Geo Frameworks, LLC, Mitchell, NE.
- AGF, 2019c. Airborne Electromagnetic Mapping and Hydrogeologic Framework of Selected Regions of the Eastern Nebraska Water Resources Assessment Area: Chapter on the Nemaha Natural Resources District. Aqua Geo Frameworks, LLC, Mitchell, NE.
- AGF, 2019d. Airborne Electromagnetic Mapping and Hydrogeologic Framework of Selected Regions of the Eastern Nebraska Water Resources Assessment Area: Chapter on the Papio-Missouri River Natural Resources District. Aqua Geo Frameworks, LLC, Mitchell, NE.
- Andersen, L.T., 2004. The Fanø Bugt Glaciotectionic Thrust Fault Complex, Southeastern Danish North Sea. A Study of Large-Scale Glaciotectionics Using High-Resolution Seismic Data and Numerical Modelling. University of Aarhus, Geological Survey of Denmark and Greenland, p. 143 report 2004/30. Geological survey of Denmark and Greenland. Ministry of the Environment.
- Antevs, E., 1929. Maps of the Pleistocene glaciations. *Bull. Geol. Soc. Am.* 40, 631–720.
- Auken, E., Boesen, T., Christiansen, A.V., 2017. Chapter two - a review of airborne electromagnetic methods with focus on geotechnical and hydrological applications from 2007 to 2017. In: Nielsen, L. (Ed.), *Advances in Geophysics*. Elsevier, pp. 47–93.
- Balco, G., Rovey, C.W., II, 2010. Absolute chronology for major Pleistocene advances of the Laurentide ice sheet. *Geology* 38, 795–798. <https://doi.org/10.1130/g30946.1>.
- Balco, G., Rovey, C.W., Stone, J.O., 2005. The first glacial maximum in North America. *Science* 307. <https://doi.org/10.1126/science.1103406>, 222–222.
- Barendregt, R.W., Duk-Rodkin, A., 2004. Chronology and extent of Late Cenozoic ice sheets in North America: a magnetostratigraphic assessment. In: Ehlers, J., Gibbard, P.L. (Eds.), *Quaternary Glaciations: Extent and Chronology. Part II: North America*. Elsevier, pp. 1–7.
- Barfod, A.A.S., Møller, I., Christiansen, A.V., 2016. Compiling a national resistivity atlas of Denmark based on airborne and ground-based transient electromagnetic data. *J. Appl. Geophys.* 134, 199–209. <https://doi.org/10.1016/j.jappgeo.2016.09.017>.
- Batchelor, C.L., Margold, M., Krapp, M., Murton, D.K., Dalton, A.S., Gibbard, P.L., Stokes, C.R., Murton, J.B., Manica, A., 2019. The configuration of Northern Hemisphere ice sheets through the Quaternary. *Nat. Commun.* 10, 3713. <https://doi.org/10.1038/s41467-019-11601-2>.

- Bennett, M.R., 2001. The morphology, structural evolution and significance of push moraines. *Earth Sci. Rev.* 53, 197–236. [https://doi.org/10.1016/S0012-8252\(00\)00039-8](https://doi.org/10.1016/S0012-8252(00)00039-8).
- Bickerdike, H.L., Evans, D.J.A., Ó Cofaigh, C., Stokes, C.R., 2016. The glacial geomorphology of the Loch Lomond Stadial in Britain: a map and geographic information system resource of published evidence. *J. Maps* 12, 1178–1186. <https://doi.org/10.1080/17445647.2016.1145149>.
- Bjornstad, B.N., Fecht, K.R., Pluhar, C.J., 2001. Long history of pre-Wisconsin, ice age cataclysmic floods: evidence from southeastern Washington state. *J. Geol.* 109, 695–713. <https://doi.org/10.1086/323190>.
- Boellstorff, J., 1978a. Chronology of some late cenozoic deposits from the central United States and the ice ages. *Trans. Nebr. Acad. Sci.* 6, 35–49.
- Boellstorff, J., 1978b. North American Pleistocene stages reconsidered in light of probable Pliocene-Pleistocene glaciation. *Science* 202, 305–307.
- Braun, D.D., 2004. The glaciation of Pennsylvania, USA. In: Ehlers, J., Gibbard, P.L. (Eds.), *Quaternary Glaciations: Extent and Chronology. Part II: North America*. Elsevier, pp. 237–242.
- Brodzikowski, K., van Loon, A.J., 1987. A systematic classification of glacial and periglacial environments, facies and deposits. *Earth Sci. Rev.* 24, 297–381. [https://doi.org/10.1016/0012-8252\(87\)90061-4](https://doi.org/10.1016/0012-8252(87)90061-4).
- Carney, C.P., Abraham, J.D., Cannia, J.C., Steele, G.V., 2015a. Airborne Electromagnetic Geophysical Surveys and Hydrogeologic Framework Development for Selected Sites in the Lower Elkhorn Natural Resources District. Exploration Resources International, Vicksburg, MS.
- Carney, C.P., Abraham, J.D., Cannia, J.C., Steele, G.V., 2015b. Final Report on Airborne Electromagnetic Geophysical Surveys and Hydrogeologic Framework Development for the Eastern Nebraska Water Resources Assessment – Volume I, Including the Lewis and Clark, Lower Elkhorn, and Papio-Missouri River Natural Resources Districts. Exploration Resources International, Vicksburg, MS, p. 132.
- Carney, C.P., Abraham, J.D., Cannia, J.C., Steele, G.V., 2015c. Final Report on Airborne Electromagnetic Geophysical Surveys and Hydrogeologic Framework Development for the Eastern Nebraska Water Resources Assessment – Volume II, Including the Lower Platte North, Lower Platte South, and Nemaha Natural Resources Districts. Exploration Resources International, Vicksburg, MS, p. 159.
- Chandler, B.M.P., Lovell, H., Boston, C.M., Lukas, S., Barr, I.D., Benediktsson, Í.Ö., Benn, D.I., Clark, C.D., Darvill, C.M., Evans, D.J.A., Ewertowski, M.W., Loibl, D., Margold, M., Otto, J.-C., Roberts, D.H., Stokes, C.R., Storrar, R.D., Stroeven, A.P., 2018. Glacial geomorphological mapping: a review of approaches and frameworks for best practice. *Earth Sci. Rev.* 185, 806–846. <https://doi.org/10.1016/j.earscirev.2018.07.015>.
- Christiansen, A.V., Auken, E., Sørensen, K., 2006. The transient electromagnetic method. In: Kirsch, R. (Ed.), *Groundwater Geophysics: A Tool for Hydrogeology*. Springer Berlin Heidelberg, Berlin, Heidelberg, pp. 179–225.
- Clark, C.D., Evans, D.J.A., Khatwa, A., Bradwell, T., Jordan, C.J., Marsh, S.H., Mitchell, W.A., Bateman, M.D., 2004. Map and GIS database of glacial landforms and features related to the last British Ice Sheet. *Boreas* 33, 359–375. <https://doi.org/10.1111/j.1502-3885.2004.tb01246.x>.
- Clark, P.U., Dyke, A.S., Shakun, J.D., Carlson, A.E., Clark, J., Wohlfarth, B., Mitrovica, J.X., Hostetler, S.W., McCabe, A.M., 2009. The last glacial maximum. *Science* 325, 710–714. <https://doi.org/10.1126/science.1172873>.
- Dellwig, F., Baldwin, A., 1965. Ice-push Deformation in Northeastern Kansas, Kansas Geological Survey Bulletin 175. part 2. Kansas Geological Survey, Lawrence, KS, p. 16.
- Divine, D.P., Joeckel, R.M., Korus, J.T., Hanson, P.R., Lackey, S.O., 2009. Eastern Nebraska water resources assessment (ENWRA): introduction to a hydrogeologic study. In: Joeckel, R.M. (Ed.), *Conservation Bulletin. Conservation and Survey Division, School of Natural Resources, Institute of Agriculture and Natural Resources, University of Nebraska-Lincoln, Lincoln, NE*, p. 31.
- Dort Jr., W., 1987. In: Johnson, W.C. (Ed.), *Salient Aspects of the Terminal Zone of Continental Glaciation in Kansas*. Kansas Geological Survey, Lawrence, KS, pp. 55–66.
- Dreeszen, V.H., 1970. The stratigraphic framework of Pleistocene glacial and periglacial deposits in the Central Plains. In: Dort, W., Knox Jones, J. (Eds.), *Pleistocene and Recent Environments of the Central Great Plains*. Department of Geology, University of Kansas, Lawrence, KS, pp. 9–22.
- Dreeszen, V.H., Burchett, R.R., 1971. Buried valleys in the lower part of the Missouri river basin. In: Bayne, C.K., O'Connor, H.G., Davis, S.N., Howe, W.B. (Eds.), *Pleistocene Stratigraphy of Missouri River Valley along the Kansas-Missouri Border*. Kansas Geological Survey, Lawrence, KS, pp. 21–25.
- Dyke, A.S., Prest, V.K., 1987. Late Wisconsinan and Holocene history of the Laurentide ice sheet. *Geogr. Phys. Quaternaire* 41, 237–263. <https://doi.org/10.7202/032681ar>.
- Ehlers, J., Gibbard, P., 2007. The extent and chronology of cenozoic global glaciation. *Quat. Int.* 164–165, 6–20. <https://doi.org/10.1016/j.quaint.2006.10.008>.
- Evans, D.J.A., Lemmen, D.S., Rea, B.R., 1999. Glacial landsystems of the southwest Laurentide Ice Sheet: modern Icelandic analogues. *J. Quat. Sci.* 14, 673–691. [https://doi.org/10.1002/\(sici\)1099-1417\(199912\)14:7<673::Aid-jqs467>3.0.Co;2-#](https://doi.org/10.1002/(sici)1099-1417(199912)14:7<673::Aid-jqs467>3.0.Co;2-#).
- Evans, D.J.A., Rea, B.R., 1999. Geomorphology and sedimentology of surging glaciers: a land-systems approach. *Ann. Glaciol.* 28, 75–82. <https://doi.org/10.3189/172756499781821823>.
- Eyles, C.H., Eyles, N., 2010. Glacial deposits. In: James, N.P., Dalrymple, R.W. (Eds.), *Facies Models 4. Geological Association of Canada*, pp. 73–104.
- Fenneman, N.M., 1946. *Physical Divisions of the United States*. U.S. Geological Survey map.
- Grosswald, M.G., Hughes, T.J., 2002. The Russian component of an arctic ice sheet during the last glacial maximum. *Quat. Sci. Rev.* 21, 121–146. [https://doi.org/10.1016/S0277-3791\(01\)00078-6](https://doi.org/10.1016/S0277-3791(01)00078-6).
- Haug, G.H., Ganopolski, A., Sigman, D.M., Rosell-Mele, A., Swann, G.E., Tiedemann, R., Jaccard, S.L., Bollmann, J., Maslin, M.A., Leng, M.J., 2005. North Pacific seasonality and the glaciation of North America 2.7 million years ago. *Nature* 433, 821–825.
- Heim, G.E., Howe, W.B., 1963. Pleistocene drainage and depositional history in northwestern Missouri. *Trans. Kans. Acad. Sci.* 378–392.
- Howe, W.B., 1968. *To Pleistocene and Pennsylvanian Formations in the St. Joseph Area, Missouri, 15th Annual Field Trip and Meeting Guidebook*. Missouri Geological Survey and Water Resources, Rolla, MO, p. 45.
- Høyer, A.-S., Jørgensen, F., Sandersen, P., Viezzoli, A., Möller, I., 2015. 3D geological modelling of a complex buried-valley network delineated from borehole and AEM data. *J. Appl. Geophys.* 122, 94–102.
- Høyer, A.-S., Lykke-Andersen, H., Jørgensen, F., Auken, E., 2011. Combined interpretation of SkyTEM and high-resolution seismic data. *Phys. Chem. Earth* 36, 1386–1397. <https://doi.org/10.1016/j.pce.2011.01.001>.
- Høyer, A.S., Jørgensen, F., Piotrowski, J.A., Jakobsen, P.R., 2013. Deeply rooted glaciotectionism in western Denmark: geological composition, structural characteristics and the origin of Varde hill-island. *J. Quat. Sci.* 28, 683–696.
- Ingólfsson, Ó., Benediktsson, Í.Ö., Schomacker, A., Kjær, K.H., Brynjólfsson, S., Jónsson, S.A., Korsgaard, N.J., Johnson, M.D., 2016. Glacial geological studies of surge-type glaciers in Iceland — research status and future challenges. *Earth Sci. Rev.* 152, 37–69. <https://doi.org/10.1016/j.earscirev.2015.11.008>.
- Jennings, C.E., Aber, J.S., Balco, G., Barendregt, R., Bierman, P.R., Rovey, C.W., Roy, M., Thorleifson, L.H., Mason, J.A., 2013. *Mid-Quaternary in North America, Encyclopedia of Quaternary Science, second ed.*, pp. 180–186.
- Johnson, W.H., Menzies, J., 2002. 10 - supraglacial and ice-marginal deposits and landforms. In: Menzies, J. (Ed.), *Modern and Past Glacial Environments*. Butterworth-Heinemann, Oxford, pp. 317–333.
- Jørgensen, F., Lykke-Andersen, H., Sandersen, P.B., Auken, E., Nørmark, E., 2003. Geophysical investigations of buried Quaternary valleys in Denmark: an integrated application of transient electromagnetic soundings, reflection seismic surveys and exploratory drillings. *J. Appl. Geophys.* 53, 215–228. <https://doi.org/10.1016/j.jappgeo.2003.08.017>.
- Jørgensen, F., Scheer, W., Thomsen, S., Sonnenborg, T.O., Hinsby, K., Wiederhold, H., Schamper, C., Burschil, T., Roth, B., Kirsch, R., Auken, E., 2012. Transboundary geophysical mapping of geological elements and salinity distribution critical for the assessment of future sea water intrusion in response to sea level rise. *Hydrol. Earth Syst. Sci.* 16, 1845–1862. <https://doi.org/10.5194/hess-16-1845-2012>.
- Kirsch, R., 2006. Petrophysical properties of permeable and low-permeable rocks. In: Kirsch, R. (Ed.), *Groundwater Geophysics: A Tool for Hydrogeology*. Springer Berlin Heidelberg, Berlin, Heidelberg, pp. 1–22.
- Kleman, J., Hattestrand, C., Borgstrom, I., Stroeven, A., 1997. Fennoscandian palaeoglaciology reconstructed using a glacial geological inversion model. *J. Glaciol.* 43, 283–299. <https://doi.org/10.1017/S0022143000003233>.
- Klint, K.E.S., Pedersen, S.A.S., 1995. The Hanklit Glaciotectionic Thrust Fault Complex, Mors, Denmark, Danmarks Geologiske Undersøgelse, Series A. Geological Survey of Denmark, Copenhagen.
- Knight, R.J., Endres, A.L., 2005. An introduction to rock physics principles for near-surface geophysics. In: Butler, D.K. (Ed.), *Near-Surface Geophysics*. Society of Exploration Geophysicists, pp. 31–70.
- Korus, J.T., 2018. Combining hydraulic Head analysis with airborne electromagnetics to detect and map impermeable aquifer boundaries. *Water* 10, 975. <https://doi.org/10.3390/w10080975>.
- Korus, J.T., Howard, L.M., Young, A.R., Divine, D.P., Burbach, M.E., Jess, J.M., Hallum, D.R., 2013. *The Groundwater Atlas of Nebraska. Third (revised) edition*. Conservation and Survey Division, School of Natural Resources, University of Nebraska-Lincoln.
- Korus, J.T., Joeckel, R.M., Divine, D.P., Abraham, J.D., 2017. Three-dimensional architecture and hydrostratigraphy of cross-cutting buried valleys using airborne electromagnetics, glaciated Central Lowlands, Nebraska, USA. *Sedimentology* 64, 553–581. <https://doi.org/10.1111/1365.12314>.
- Leighton, M.M., 1959. Stagnancy of the illinoian glacial lobe east of the Illinois and Mississippi rivers. *J. Geol.* 67, 337–344. <https://doi.org/10.1086/626587>.
- Leighton, M.M., Brophy, J.A., 1961. Illinoian glaciation in Illinois. *J. Geol.* 69, 1–31. <https://doi.org/10.1086/626713>.
- Lugn, A.L., 1935. *The Pleistocene Geology of Nebraska*. Nebraska Geological Survey Bulletin 10. Conservation and Survey Division. University of Nebraska-Lincoln, Lincoln, NE, p. 223.
- Luman, D.E., Smith, L.R., Goldsmith, C.C., 2002. *Illinois Surface Topography, Illinois Map 11*. Illinois State Geological Survey, Champaign, IL.
- Margold, M., Stokes, C., Clark, C., 2018. Reconciling records of ice streaming and ice margin retreat to produce a palaeogeographic reconstruction of the deglaciation of the Laurentide Ice Sheet. *Quat. Sci. Rev.* 189. <https://doi.org/10.1016/j.quascirev.2018.03.013>.
- Oldenborger, G.A., Pugin, A.J.-M., Pullan, S.E., 2013. Airborne time-domain electromagnetics, electrical resistivity and seismic reflection for regional three-dimensional mapping and characterization of the Spiritwood Valley Aquifer, Manitoba, Canada. *Near Surf. Geophys.* 11, 63–74. <https://doi.org/10.3997/1873-0604.2012023>.
- Paine, J.G., Minty, B.R., 2005. Airborne hydrogeophysics. In: Rubin, Y., Hubbard, S.S. (Eds.), *Hydrogeophysics*. Springer, Dordrecht, The Netherlands, pp. 333–357.
- Palacky, G., 1988. Resistivity characteristics of geologic targets. In: Nabighian, M.N. (Ed.), *Electromagnetic Methods in Applied Geophysics*. Society of Exploration Geophysicists, Tulsa, Oklahoma, pp. 53–129.
- Pedersen, S.A.S., 1996. Progressive glaciotectionic deformation in Weichselian and Paleogene deposits at Feggeklit, northern Denmark. *Bull. Geol. Soc. Den.* 42, 153–174.

- Pedersen, S.A.S., 2005. Structural analysis of the Rubjerg Knude glaciotectionic complex, Vendsyssel, northern Denmark. *Geol. Surv. Den. Greenl. Bull.* 8, 1–192.
- Prest, V.K., Grant, D.R., Rampton, V.N., 1968. *Glacial Map of Canada*, Map 1253A. Geological Survey of Canada.
- Prior, J.C., 1976. *A Regional Guide to Iowa Landforms*, Educational Series. Iowa Geological Survey, Iowa City, Iowa, p. 72.
- Ramage, J.M., Gardner, T.W., Sasowsky, I.D., 1998. Early Pleistocene glacial lake lesley, west branch susquehanna river valley, central Pennsylvania. *Geomorphology* 22, 19–37. [https://doi.org/10.1016/S0169-555X\(97\)00053-6](https://doi.org/10.1016/S0169-555X(97)00053-6).
- Räsänen, M., Auri, J., Huittinen, J., Klap, A., Virtasalo, J., 2009. A shift from lithostratigraphic to allostratigraphic classification of Quaternary glacial deposits. *GSA Today (Geol. Soc. Am.)* 19, 4–11.
- Reed, E.C., Dreeszen, V.H., 1965. Revision of the Classification of the Pleistocene Deposits of Nebraska. Geological Survey Bulletin 23. Conservation and Survey Division, University of Nebraska-Lincoln, Lincoln, NE, p. 65.
- Robinson, D.A., Binley, A., Crook, N., Day-Lewis, F.D., Ferre, T.P.A., Grauch, V.J.S., Knight, R., Knoll, M., Lakshmi, V., Miller, R., Nyquist, J., Pellerin, L., Singha, K., Slater, L., 2008. Advancing process-based watershed hydrological research using near-surface geophysics: a vision for, and review of, electrical and magnetic geophysical methods. *Hydrol. Process.* 22 (18), 3604–3635. <https://doi.org/10.1002/hyp.6963>.
- Rovey, C.W., Bettis, E., 2014. Pleistocene geology and classic type sections along the Missouri River valley in western Iowa. In: Korus, J.T. (Ed.), *Geologic Field Trips along the Boundary between the Central Lowlands and Great Plains*. The Geological Society of America, Boulder, CO, pp. 23–38.
- Roy, M., Clark, P.U., Barendregt, R.W., Glasmann, J.R., Enkin, R.J., 2004. Glacial stratigraphy and paleomagnetism of late Cenozoic deposits of the north-central United States. *Geol. Soc. Am. Bull.* 116, 30–41. [10.1130/B25325.1](https://doi.org/10.1130/B25325.1) *J. Geol.*
- Sharpe, D., Pugin, A., Pullan, S., Gorrell, G., 2003. Application of seismic stratigraphy and sedimentology to regional hydrogeological investigations: an example from Oak Ridges Moraine, southern Ontario, Canada. *Can. Geotech. J.* 40, 711–730.
- SkyTEM, 2018. SkyTEM Geophysical Survey Systems. <http://skytem.com/tem-systems/>. (Accessed 2 October 2019).
- Soller, D.R., 1992. Text and references to accompany "Map showing the thickness and character of Quaternary sediments in the glaciated United States east of the Rocky Mountains", U.S. Geological Survey Bulletin 1921. U.S. Geological Survey 54.
- Sollid, J.L., Sørbel, L., 1994. Distribution of glacial landforms in southern Norway in relation to the thermal regime of the last continental ice sheet. *Geogr. Ann. Phys. Geogr.* 76, 25–35. <https://doi.org/10.2307/521317>.
- Sørensen, K.I., Auken, E., 2004. SkyTEM—a new high-resolution helicopter transient electromagnetic system. *Explor. Geophys.* 35, 194–202.
- Stanley, K.O., 1974. Morphology and hydraulic significance of climbing ripples with superimposed micro-ripple-drift cross-lamination in lower Quaternary lake silts, Nebraska. *J. Sediment. Res.* 44, 472–483. <https://doi.org/10.1306/74d72a63-2b21-11d7-8648000102c1865d>.
- Stiff, B.J., Hansel, A.K., 2004. Quaternary glaciations in Illinois. In: Ehlers, J., Gibbard, P.L. (Eds.), *Quaternary Glaciations: Extent and Chronology. Part II: North America*. Elsevier, pp. 71–82.
- Swinehart, J.B., Dreeszen, V.H., Richmond, G.M., Tipton, M.J., Bretz, R.F., Steece, F.V., Hallberg, G.R., Goebel, J.E., 1994. Quaternary geologic map of the Platte River 4 degrees x 6 degrees quadrangle, United States. In: Goebel, J.E., Richmond, G.M. (Eds.), *Map I-1420 (NK-14)*. U.S. Geological Survey.
- Syverson, K.M., Colgan, P.M., 2011. The quaternary of Wisconsin: an updated review of stratigraphy, glacial history and landforms. In: Ehlers, J., Gibbard, P.L., Hughes, P.D. (Eds.), *Quaternary Glaciations: Extent and Chronology*. Elsevier, pp. 537–552.
- Szabo, J.P., Chanda, A., 2004. Pleistocene glaciation of Ohio, USA. In: Ehlers, J., Gibbard, P.L. (Eds.), *Quaternary Glaciations: Extent and Chronology. Part II: North America*. Elsevier, pp. 233–236.
- Todd, J.E., 1911. History of Wakarusa Creek. *Transactions of the Kansas Academy of Science*, pp. 211–218.
- Viezzoli, A., Christiansen, A.V., Auken, E., Sørensen, K., 2008. Quasi-3D modeling of airborne TEM data by spatially constrained inversion. *Geophysics* 73, F105–F113. <https://doi.org/10.1190/1.2895521>.
- Wayne, W.J., 1985. Drainage patterns and glaciations in eastern Nebraska. In: Dort Jr, W. (Ed.), *Institute for Tertiary-Quaternary Studies - Ter-Qua Symposium Series*. Nebraska Academy of Sciences, Lincoln, NE, pp. 111–117.
- Willard, J.E., 1980. Regional Directions of Ice Flow along the Southwestern Margin of the Laurentide Ice Sheet as Indicated by Distribution of Sioux Quartzite Erratics. Department of Geology. University of Kansas, Lawrence, KS, p. 87.
- Witzke, B.J., Ludvigson, G.A., 1990. Petrographic and stratigraphic comparisons of sub-till and inter-till alluvial units in western Iowa; implications for development of the Missouri River drainage. In: Bettis, E.A.I. (Ed.), *Holocene Alluvial Stratigraphy and Selected Aspects of the Quaternary History of Western Iowa*. Iowa Geological Survey, Iowa City, IA, pp. 119–143.